Dynamic Network Reconstruction from Gene Expression Data Describing the Effect of LiCl Stimulation on Hepatocytes

Sebastian Zellmer[1,*], Wolfgang Schmidt-Heck[2], Frank Gaunitz[3], Alicja Baldysiak-Figiel[1], Reinhardt Guthke[2], Rolf Gebhardt[1]

[1]Institute of Biochemistry, Medical Faculty, University Leipzig, Johannisallee 30, 04103 Leipzig, Germany
[2]Leibniz-Institute for Natural Product Research and Infection Biology - Hans-Knoell-Institute (HKI), Beutenbergstrasse 11a, 07745 Jena
[3]Interdisciplinary Center for Clinical Research Leipzig (IZKF), Inselstrasse 22, 04103 Leipzig

Summary

Wnt/ß-catenin signalling plays an important role in zonation of liver parenchyma and in patterning of hepatocyte heterogeneity. A characteristic marker of this heterogeneity is glutamine synthetase, which is expressed only in a subset of pericentrally located hepatocytes. To investigate, whether and how the Wnt/β-catenin signalling pathway is involved a culture of hepatocytes was stimulated by LiCl. This resulted in an increase in the specific GS activity, indicating that the Wnt/β-catenin pathway may participate in regulating GS levels. Affymetrix GeneChip oligonucleotide arrays were used to monitor the gene expression changes during a period from 2 to 24 hours after stimulation by LiCl. Samples from a cultivation without stimulation were used as controls. Based on the gene expression profiles a hypothetic signal transduction network was constructed by a reverse engineering algorithm. The network robustness was tested and the most stable structure was identified.

1   Introduction

The liver is the main organ of intermediary metabolism. It consists of hepatocytes (60% of all cells and 80 % of the liver volume), endothelial cells (15-20 %), Kupffer cells and Ito cells. The smallest structural and functional unit in the liver is the lobulus. Within the lobulus the hepatocytes are arranged in a spatial organization, related to the afferent and efferent blood vessels. Accordingly, they are referred to periportal and pericentral hepatocytes, respectively. Periportal and pericentral cells differ in the metabolic capacity and, as a consequence, in the enzyme/protein expression pattern [1]. Glutamine synthetase (GS), for example, is expressed only in a subset of pericentral hepatocytes and can be used as a selective marker for pericentral cells. Factors responsible for the induction and regulation of GS expression have been described, but the mechanism of regulation has not been identified in detail yet.

Experimental evidence exists that the Wnt/β-catenin signalling pathway plays an important role in the zonation of liver parenchyma and for the expression of GS. Within the Wnt/β-catenin signalling pathway glycogen synthase kinase-3β (GSK3β) is a central mediator. GSK3β is associated with several other regulatory proteins, including adenomatous polyposis coli (APC) and axin, which built the so-called destruction complex. In the unstimulated

---

[*] Corresponding author

hepatocyte β-catenin is located close to the cell membrane and fulfills structural tasks. The cytoplasmatic concentration of free β-catenin is low, since free β-catenin is bound to the destruction complex and rapidly phosporylated at N-terminal serine and threonin residues by GSK3β. The phosphorylated β-catenin is then subjected to proteasome-mediated degradation.

An activation of the Wnt/β-catenin pathway (e.g. by Wnt factors) results in an inhibition of GSK3β and free, unphosphorylated β-catenin accumulates in the cytoplasm. It translocates into the nucleus and induces the expression of LEF/TCF (lymphoid-enhancing factor/T-cell factor 1) depending target genes.

Recently it has been shown that mutations in the APC or the β-catenin gene severely disturbs liver zonation. These mutations can result in a homogenous expression of GS within the liver parenchyma [2]. The authors concluded that the expression of GS is regulated partially by the Wnt/β-catenin pathway. This conclusion is also favoured by data from liver tumours [3]. Previously it has been shown that a soluble polypeptide factor can induce glutamine synthetase in vitro [4] and recent data show that this factor is most likely related to the Wnt/β-catenin pathway [5].

However, in vivo, the situation seems to be more complex. From the scarce literature data can be concluded that it takes weeks or months until mutations in the β-catenin pathway result in an increased expression of GS. Therefore it is likely that the induction of GS is additionally regulated by different factors like cell-matrix interactions and/or the hepatocyte cell cycle.

LiCl is a well known inhibitor of the GSK3β. Several groups have shown that the incubation of cells with LiCl in millimolar concentrations results in an inhibition of GSK3β. In the present study we investigated the effects of LiCl on the expression of GS in hepatocytes and tried to characterize possible regulatory factors/pathways.

2   Material and methods

HepG2 cells were obtained from ECACC (http://www.ecacc.org.uk). Cell culture material was obtained from TPP (Trasadingen, Switzerland). LiCl was a product of Merck (Darmstadt, Germany), glutamine was obtained from Roth (Karlsruhe, Germany), penicillin and streptomycin was from Sigma (Taufkirchen, Germany). DMEM and FCS were purchased from PAA Laboratories (Cölbe, Germany). In all experiments HepG2 cells were cultivated in DMEM supplemented with 10 % FCS, 2 mM glutamine and penicillin/streptomycin. For the isolation of mRNA the cells were harvested using Accutase (PAA Laboratories) and plated at a density of 2.5×10^6 cells / culture dish (90 mm) in 7.5 ml medium. Incubation with DMEM, containing 50 mM LiCl was started 22 h later. Cells were harvested before the addition of LiCl and 2, 4, 8, 12 and 24 h later and the mRNA was isolated using the RNeasy Mini kit (Qiagen, Hilden, Germany).

For Northern blot analysis cells were grown under the same conditions as for gene chip analysis and two dishes for each mRNA preparation were used. The blotting was performed according to standard protocols [6]. For the hybridisation a digoxigenin labelled probe from the rat GS gene was used and a quantitative analysis of the mRNA was performed using the Phoretix 1D Quantifier software (Phoretix International, Newcastle, UK).

Cell viability was tested using the MTT assay. Briefly, 0.63×10^6 cells per cm^2 were seeded in 24-well plates. The next day cells were incubated with LiCl for 24 h, followed by an incubation with 0.5 mg/ml MTT reagent (Sigma, Taufkirchen) for 2 h. Cells were lysed using DMSO and the absorbance in each well was determined at 590 nm using a Spectrafluor plate

reader (Tecan GmbH, Crailsheim, Germany). The absorbance of the untreated control was set to 100 % viability.

Determination of GS activity was performed by the method of Levintow [7] with the modifications described by Gebhardt and Williams [8]. Briefly, cells were cultivated as described above, harvested in Hanks balanced solution using a rubber policeman and homogenized by sonication (Sonopuls, Bandelin, Berlin, Germany). Then, 100 µl of the homogenate was used for the GS activity assay and the absorbance was determined at 540 nm.

Protein concentration was determined using the Bradford assay [9] and the specific GS activity of each sample was expressed in mU/mg.

For the expression analysis Affymetrix (Affymetrix Inc., USA) genechips HG-U133A and U95 were used with 22.283 and 12.651 probesets, respectively. The gene expression data were pre-processed using 'affyPLM' packages of the Bioconductor Software [10, 11]. The log-ratios of expression values from samples with and without LiCl stimulation were calculated after normalization by Probe-level Linear Models. Probesets representing differentially expressed genes were selected by the following criteria: i) the fold change exceeds the threshold 1.62 (justification see below) for 2 h, 4 h of 8 h after stimulation and ii) there is a direct or indirect link to the Wnt/ß-catenin pathway or to the GS induction described in literature. The threshold for the minimum fold change required for differentially expressed genes was identified from the log-ratios of the U133A and the U95 expression data. Processing and visualization of data were performed using MATLAB tools (The MathWorks Inc., Natick, MA).

The reverse engineering algorithm [12] was used to identify the parameters of the following linear differential equation system network model

$$\frac{dx_i(t)}{dt} = \sum_{j=1}^{C} w_{i,j} \cdot x_j(t) + b_i \cdot u(t) \qquad (1)$$

in which $x_i(t)$ is the expression of gene $i = 1,...,C$ at time t, $w_{i,j}$ denotes the gene-gene interactions and b_i represents the stimulus-gene interactions. The number of model variables $C = K + 2$, where K is the number of differentially expressed genes selected as described above. Beside these expression profiles of the K genes the expression profile of GLUL and the time course of the specific GS activity were included into the set of C model variables. The pulse function $u(t)$ was defined as $u(0 \leq t \leq t_1) = 1$ and $u(t_1 < t < 0) = 0$, i.e. the influence of stimulus LiCl is taken to be constant over a time t_1 (2 hours). In addition, the system is assumed to be at equilibrium prior to stimulation, i.e. $dx_i(t<0)/dt = x_i(t<0) = 0$.

The reverse engineering algorithm [12] minimized the mean square error of the model fit to the log ratio of gene expression data $X_j(t_i)$ as well as the number of non-zero parameters $w_{i,j}$ and b_i. The mean square error represented the squared and summarized difference between the simulated kinetics $x_j(t)$ at the sample time $t=t_i$ and measured gene expression profile data $X_j(t_i)$.

In order to identify the most robust model different combination of models were generated and analyzed using the following procedure. The models were generated by varying the reverse engineering algorithm's configuration and by disturbing the input data $X_j(t_i)$. The algorithm can be configured by pre-setting some interactions. Direct interactions from LiCl to the variables GLUL and GS were excluded. Direct interactions from LiCl to the K genes were pre-set in the following manner. In the first step of search for robust structures k stimulus-gene interactions were pre-set between the stimulus LiCl and a sub-set of k genes taken from the K genes, whereas the other C-k stimulus-gene interactions were excluded as direct

interactions. The number of N_K combinations of k variables (k=1,..., K) taken from the set of K genes is:

$$N_K = \sum_{k=1}^{K} \frac{K!}{k! \cdot (K-k)!} \qquad (2)$$

For each configuration the reverse engineering algorithm was run 50 times thereby disturbing the input data randomly by adding normally distributed noise with a mean of zero and a standard deviation (SD) of 0.05 to the measured data. A gene-to-gene interaction was accepted in the model if it occurred at least 40 times (80%). For each selected gene i (i=1,...,C) the numbers of stable gene-gene interactions (i) were summarized over the K_C models and called N_i.

In the second step of search for robust structures the stimulus-gene interactions from LiCl to the three genes with the highest N_i were pre-set, whereas the other C-3 stimulus-gene interactions were excluded as direct interactions. To validate the received model the reverse engineering algorithm was applied 1000 times using normally distributed noise with a mean of zero and standard deviations of 0.05 added to the log ratios. A gene-gene interaction was accepted in the recalculated network, if it occurred in at least 80 percent of the reconstructed models.

3   Results

At first the toxicity of LiCl was studied. Cells were incubated with concentrations up to 500 mM LiCl for 24 h and the toxicity was determined using the MTT assay (Fig. 1). At a concentration of 125 mM LiCl the viability started to decrease and at 250 mM all cells were dead. However, even at concentrations below 125 mM (e.g. 100 mM) changes in the morphology of the cells occurred (not shown). Therefore, we decided to use 50 mM LiCl in all further experiments, which induced no visible change in the morphology of the cells.
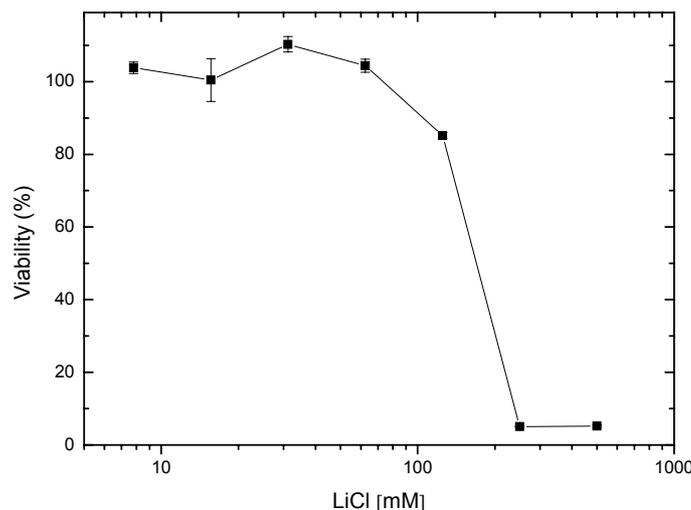

Fig. 1: Effect of LiCl on the viability of HepG2 cells. Each point represents the mean and the SD of 3 determinations.

Fig. 2 shows that there is a concentration dependent increase in the specific GS activity from a basal level of 41 ± 1.4 mU/mg up to 74 ± 4.5 mU/mg after the incubation with 50 mM LiCl

for 24 h. This suggests that the Wnt/β-catenin pathway might be involved in the regulation of the GS expression.
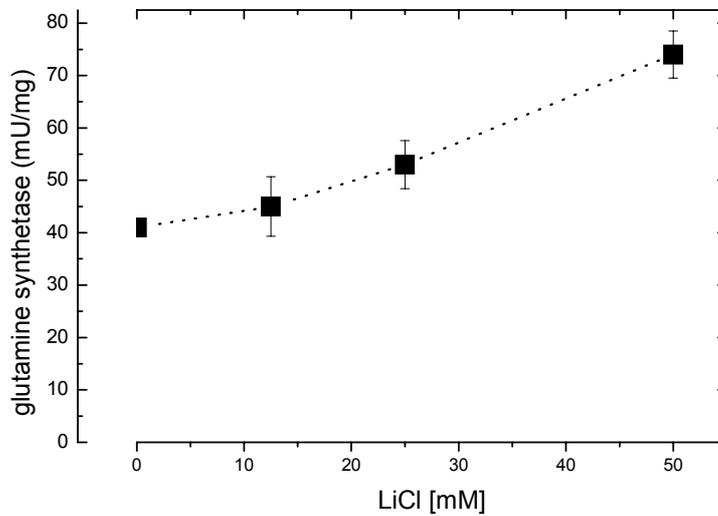

Fig. 2: Effect of the LiCl concentration on the specific activity of glutamine synthetase after 24 h of incubation. Each point represents the mean and the SD of 3 determinations.

Next we studied the time course of the induction. After addition of LiCl cells were harvested after 2, 4, 8, 12, 24, 32 and 48 h. Figure 3 shows that the specific GS activity increased over the first 4 h and reached a constant level after 8-12 h. In order to prove, whether similar changes are detectable on the level of the mRNA, gene chip analysis and Northern Blot experiments were performed.
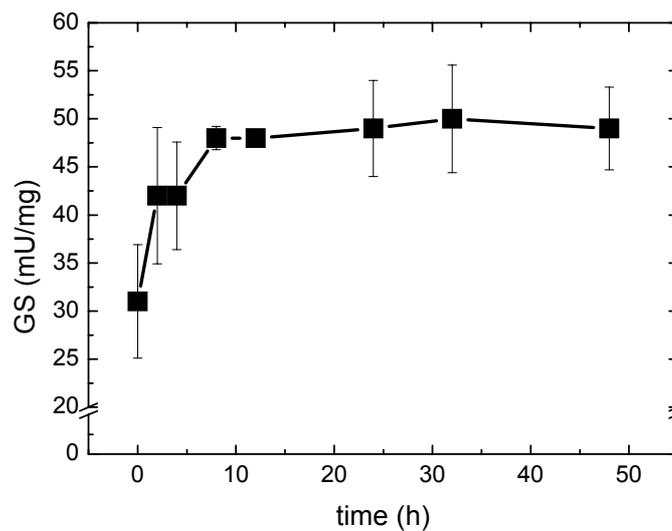

Fig. 3: Effect of the incubation time on the specific GS activity using 50 mM LiCl. Each point represents the mean and the SD of 3 determinations.

Fig. 4 shows the expression profile of the GS mRNA on the Affimetrix gene chip HG-U133A. The maximum of expression occurred 12 h after the addition of 50 mM LiCl to the cells. A similar time course was obtained from Northern Blot analysis (data not shown). Therefore, it can be concluded that the increase of the specific GS activity is based on an increase in mRNA.
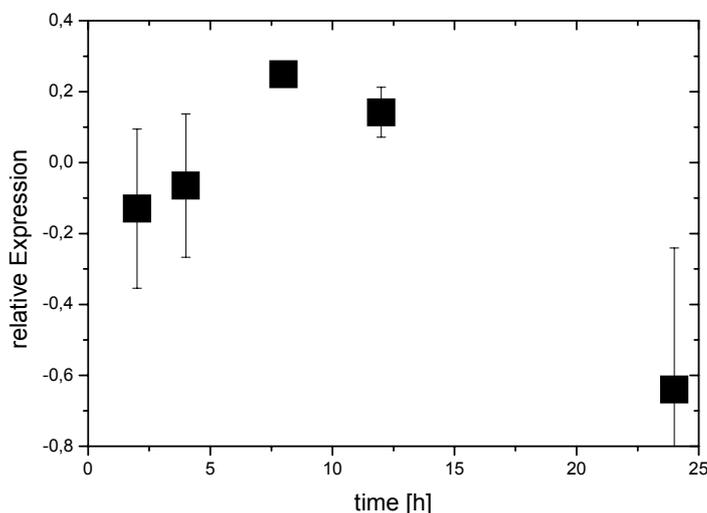

Fig. 4: Effect of the LiCl incubation time on the expression of GS mRNA (GLUL), determined using the HG-U133A gene chip. A maximum of the expression is detected after 8 h. Each point represents the mean and the SD of the 3 probesets for the gene GLUL.
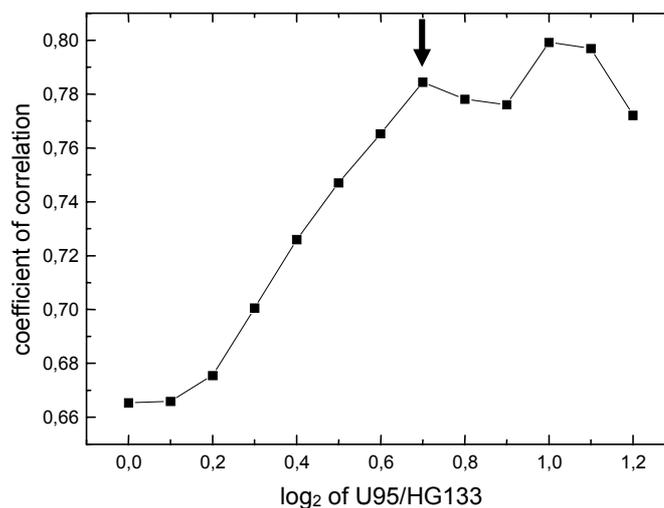

Fig. 5: Relationship between differentially expressed genes and the correlation of detection using the HG-U133A and the U95 gene chips. The arrow indicates the 1.62fold increased expression.

In order to determine factors involved in the regulation of GS expression after the addition of LiCl, gene chip analysis was performed. First of all the reproducibility of the experimental setup and the analysis was tested. Two different Affimetrix gene chips (HG-U133A and U95)

and two mRNA preparations from two different cell culture passages were compared. All up- or down-regulated genes were identified for each time-point. After plotting the $\log_2$ ratio of these genes against the correlation coefficient of the second chip analysis, a local maximum of was detected at 0.7. Thus, the threshold of significantly expressed genes was set to 1.62fold ($= \log_2 (0.7)$). This threshold was used for the further identification of differentially expressed genes (Fig. 5).

Fold +/-	ID	Symbol	Description
2.581	201289_at	CYR61	cysteine-rich, angiogenic inducer, 61
2.319	201631_s_at	IER3	immediate early response 3
2.233	210764_s_at	CYR61	cysteine-rich, angiogenic inducer, 61
2.132	202887_s_at	DDIT4	DNA-damage-inducible transcript 4
2.047	222018_at	NACA	nascent-polypeptide-associated complex α polypeptide
1.972	221989_at	RNU70	RNA, U70 small nucleolar
1.812	202302_s_at	FLJ11021	similar to splicing factor, arginine/serine-rich 4
1.738	222040_at	-	-
1.714	209774_x_at	CXCL2	chemokine (C-X-C motif) ligand 2
1.684	205822_s_at	HMGCS1	3-hydroxy-3-methylglutaryl-Coenzyme A synthase 1
1.675	214837_at	ALB	albumin
1.653	212434_at	GRPEL1	GrpE-like 1, mitochondrial (E. coli)
1.652	201464_x_at	JUN	v-jun sarcoma virus 17 oncogene homolog (avian)
1.649	204847_at	ZNF-U69274	zinc finger protein
1.643	200779_at	ATF4	activating transcription factor 4
1.623	209647_s_at	SOCS5	suppressor of cytokine signalling 5

Table 1a. Genes significantly up-regulated 2 h after the addition of 50 mM LiCl.

Analysis of the data showed that during the cultivation a significant change in the expression of genes occurred in un-stimulated cells. Therefore, only the expression of the LiCl treated and untreated samples of the same time-point were compared. Table 1 shows the genes differentially expressed, 2 h after the addition of LiCl. It resulted in an up-regulation of 16 genes, including cystein-rich angiogenic inducer 61 (Cyr61, 2.58fold). Also, 21 genes were significantly downregulated (Table 1b), which include CCAAT/enhancer binding protein β (C/EBPβ, 1.98fold), insulin-like growth factor binding protein 1 (IGFBP1, 2.07fold), TGFβ-induced factor (TGIF, 1.80fold).

Fold +/-	ID	Symbol	Description
-2.065	205302_at	IGFBP1	insulin-like growth factor binding protein 1
-1.984	212501_at	CEBPB	CCAAT/enhancer binding protein (C/EBP), beta
-1.960	209112_at	CDKN1B	cyclin-dependent kinase inhibitor 1B (p27, Kip1)
-1.850	213390_at	C19orf7	chromosome 19 open reading frame 7
-1.804	203313_s_at	TGIF	TGFB-induced factor (TALE family homeobox)
-1.786	218897_at	MGC10993	hypothetical protein MGC10993
-1.752	203574_at	NFIL3	nuclear factor, interleukin 3 regulated
-1.751	200768_s_at	MAT2A	methionine adenosyltransferase II, alpha
-1.743	220491_at	HAMP	hepcidin antimicrobial peptide
-1.724	214657_s_at	TncRNA	trophoblast-derived noncoding RNA
-1.715	213019_at	RANBP6	RAN binding protein 6

-1.711	203380_x_at	SFRS5	splicing factor, arginine/serine-rich 5
-1.710	204524_at	PDPK1	3-phosphoinositide dependent protein kinase-1
-1.684	203739_at	ZNF217	zinc finger protein 217
-1.680	205749_at	CYP1A1	cytochrome P450, family 1, subfamily A, polypeptide 1
-1.670	209681_at	SLC19A2	solute carrier family 19 (thiamine transporter), member 2
-1.667	202431_s_at	MYC	v-myc myelocytomatosis viral oncogene homolog (avian)
-1.663	214670_at	ZNF36	zinc finger protein 36 (KOX 18)
-1.649	211297_s_at	CDK7	cyclin-dependent kinase 7
-1.623	209102_s_at	HBP1	HMG-box transcription factor 1
-1.622	218185_s_at	FLJ10511	armadillo repeat containing protein

Table 1b. Genes significantly down-regulated 2 h after the addition of 50 mM LiCl.

Incubation of hepatocytes with 50 mM LiCl for 4 h resulted in an up-regulation of 43 genes (Fig. 6), including the dishevelled associated activator of morphogenesis 1 (DAAM1, 1.71fold). The latter is a known factor of the Wnt/β-catenin pathway. In addition, factors of the TGFβ pathway are up-regulated, including follistatin (FST, 1.97fold) and thrombospondin 1 (THBS1, 2.1fold). Cyr61, which was up-regulated after 2 h remained up-regulated 2.30fold. At the same time-point 128 genes are down-regulated. Among them are several genes which encode factors that are involved in the Wnt/β-catenin pathway, like frizzled homolog 4 (FZD4, 1.98fold) and dickkopf homolog 1 (DKK-1, 1.86fold).
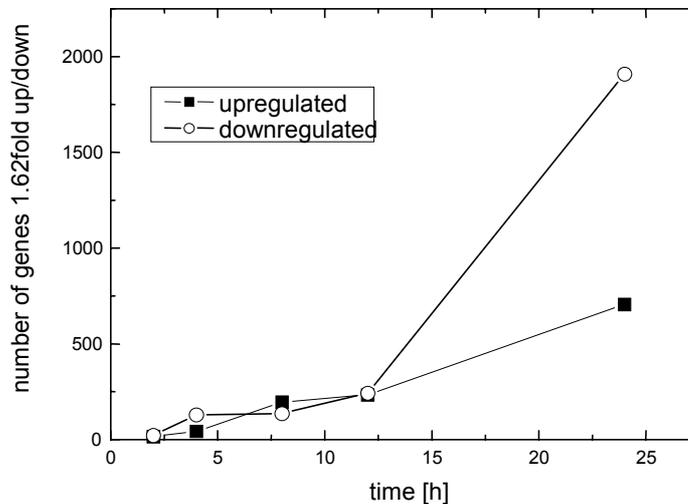

Fig. 6: The number of differentially expressed genes on the HG-U133A gene chip. Cells were incubated with 50 mM LiCl for 24 h and the detection level for differential expression was set to 1.62fold.

The increase in GS mRNA had a local maximum after 8-12 h (Fig. 4). Therefore, it was concluded that signals involved in the induction of GS should occur within the first eight hours after the addition of LiCl. There is increasing evidence in the literature, that the Wnt/β-catenin pathway is involved in the regulation of the GS expression. Therefore, significantly up- or down-regulated genes of the Wnt/β-catenin pathway or genes known to be involved in the regulation of GS were chosen for further analysis. These genes were grouped into 8

clusters, characterized by similar expression profiles. For each cluster one representative gene was selected as shown in Table 2.

representative gene	time points of significant up- or down regulation	number of genes in the cluster
CYR61	2h, 4h, 8h, 12h, 24h up	2
FZD4	4h, 12h, 24h down	14
C/EBPα	8h, 12h, 24h down	49
IGFBP1	2h down	5
DKK-1	4h down	20
DAAM1	4h, 8h up, 24h down	1
FST	8h, 12h, 24h up	28
THBS1	4h up	7

Tab. 2: Representative genes of the clusters used for model calculation

For the calculation of the network describing the effect of LiCl on the expression of GS, the expression profiles of the 8 selected genes (Table 2), the expression profile of GLUL (from Northern Blot) and the time course of the specific GS activity (Fig. 3) was used. In the first search for a robust network model the reverse engineering algorithm [12] was applied 12,750 times, i.e. for $N_K = 255$ configurations with all combinations of the pre-set stimulus-gene interactions from LiCl to one or more of the 8 selected genes and repeated 50 times each with randomly disturbed input data. As shown in Figure 7 the most stable models consisted of a LiCl-to-IGFBP1 interaction, followed by a LiCl-to-DKK-1 and a LiCl-to-FZD4 interaction. These three most stable LiCl-to-gene interactions were pre-set in the reverse engineering algorithm's configuration for the second search of the most robust model.
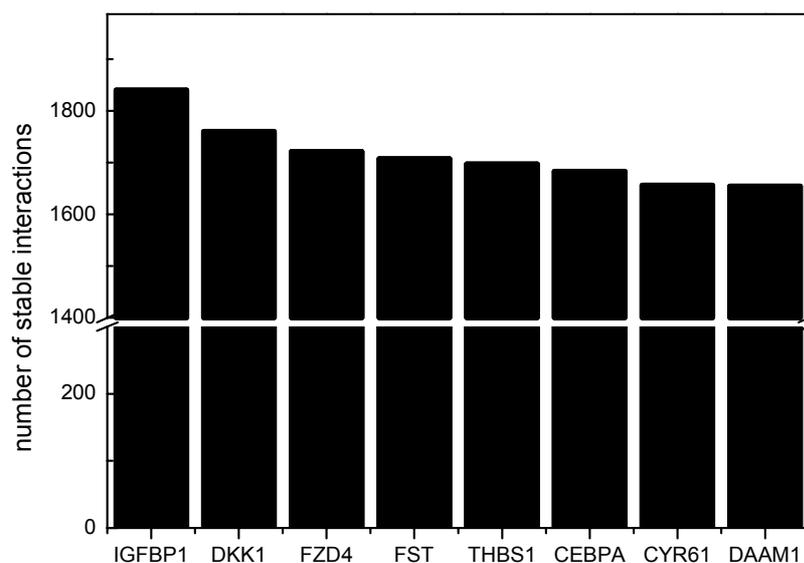

Fig. 7: Number of stable LiCl-gene interactions in 255 possible models (=N_K, see text)

Fig. 8 and equations 1-10 (Box 1) represent the model generated by the algorithm configured as described and applied to undisturbed data. This model describes the effect of LiCl on the expression of glutamine synthetase. LiCl seems to have a direct inhibitory effect on the expression of IGFBP1 (insulin-like growth factor binding protein 1), FZD4 (frizzled homolog 4) and DKK-1 (Dickkopf-1). The model also shows that DKK-1 inhibits the expression of GLUL and that the expression of the GLUL mRNA is directly linked to the specific GS activity. The results of the model fit are shown also in Fig. 9, where dots represent the measured data. As can be seen from the time course of the expression data a rise of GLUL expression follows a decrease of DKK-1 expression after a short delay. In addition, the specific enzyme activity of GS increases with a short delay after the increase in the GS mRNA (GLUL).

$$\frac{dx_1}{dt} = -4.17 \cdot x_1 - 7.50 \cdot x_6$$

$$\frac{dx_2}{dt} = -0.53 \cdot x_2 - 2.42 \cdot x_6 - 1.79 \cdot u(t)$$

$$\frac{dx_3}{dt} = 0.01 \cdot x_1 - 0.30 \cdot x_2$$

$$\frac{dx_4}{dt} = -0.38 \cdot x_4 - 0.48 \cdot x_6$$

$$\frac{dx_5}{dt} = -0.46 \cdot x_4 - 0.51 \cdot x_6$$

$$\frac{dx_6}{dt} = -0.64 \cdot x_6 - 0.54 \cdot u(t)$$

$$\frac{dx_7}{dt} = 0.53 \cdot x_2 - 0.79 \cdot x_7 - 0.20 \cdot u(t)$$

$$\frac{dx_8}{dt} = 0.42 \cdot x_6 - 0.29 \cdot x_8$$

$$\frac{dx_9}{dt} = -0.38 \cdot x_2 - 0.75 \cdot x_7 - 0.10 \cdot x_9$$

$$\frac{dx_{10}}{dt} = 0.84 \cdot x_9$$

Box 1: Equations describing the structure of the generated network (Fig. 8) in detail. The variables x_1, . . . , x_9 are the log-ratios of CYR61, IGFBP1, DAAM1, FST, THBS1, FZD4, DKK-1, CEBPA and GLUL, respectively. The variable x_{10} is the specific enzyme activity of the glutamine synthetase (GS).
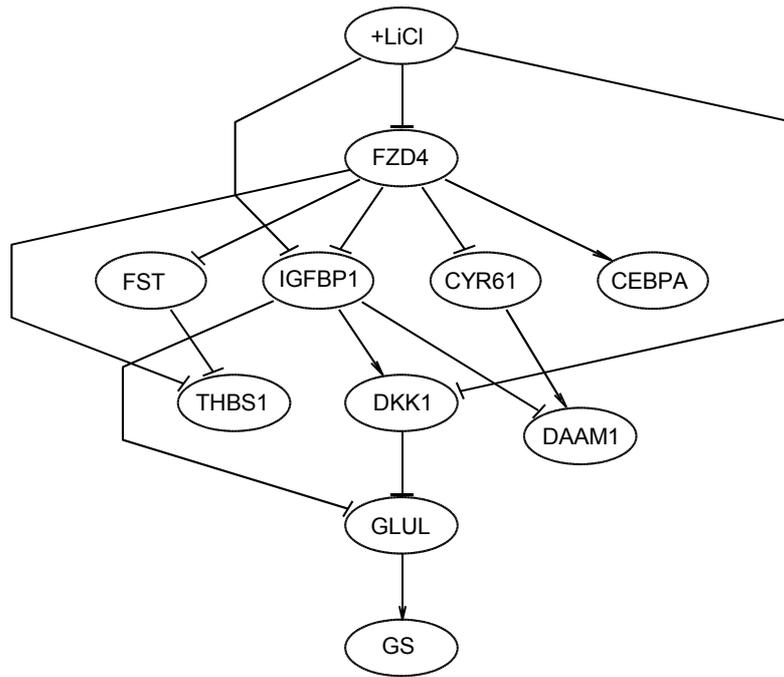
Fig.8: Model for the effect of LiCl on the increased expression of GS. Measured data of eight significantly expressed genes from the gene chip analysis and the expression data of GLUL (from the Northern blot) and the time course of the specific GS activity were used for the calculation of the network. CEBPA: C/EBPα; Cyr61: Cystein-rich protein, DAAM1: dishevelled associated activator of morphogenesis; DKK1: Dickkopf-1; FST: Follistatin, FZD4: frizzled homolog 4; GLUL: glutamine synthetase; IGFBP1: Insulin-like growth factor binding protein 1; THBS1: thrombospondin.
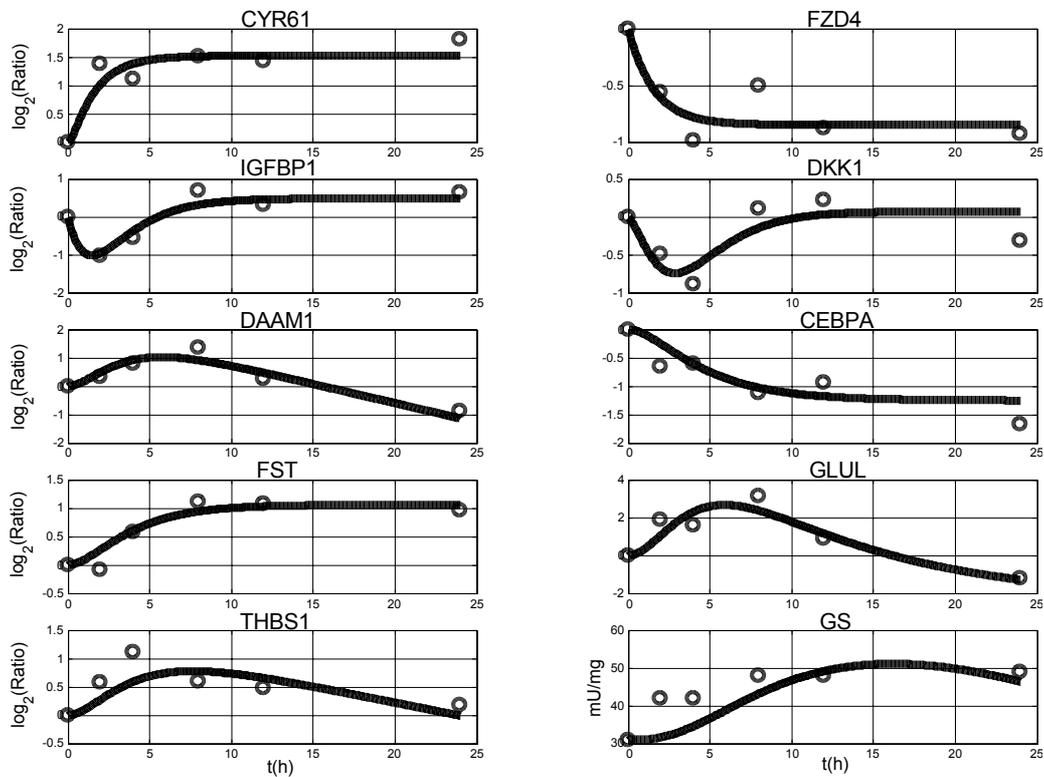

Fig. 9. Measured (dots) and simulated expression kinetic (lines) for the selected genes as well as the specific GS activity.

In order to validate the obtained model it was recalculated 1000 times adding noise with a standard deviation of 0.05 to the measured data. A gene-to-gene interaction was accepted in this calculation, if it occurred in at least 80 percent of the reconstructed models. Fig. 10 shows the result of this validation. Six gene-to-gene interactions were stable, represented by thick lines and 5 gene-to-gene interactions were unstable (thin lines). The DKK-1-GLUL interaction and the LiCl-IGFBP1 interaction are stable, indicating that these interactions are very likely to occur. The fitted curves and the measured data of the stable model are shown in Figure 11. In this recalculated model DAAM1 and THBS1 were set to zero. Therefore, no lines are present in the corresponding graph.
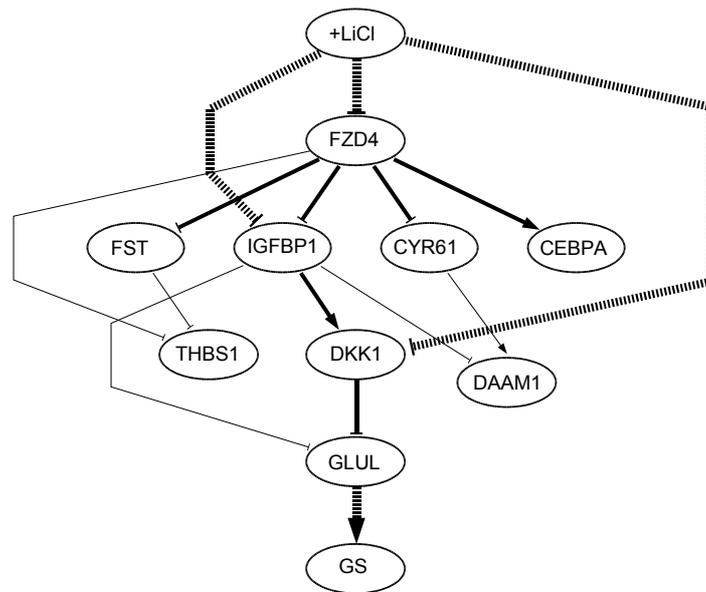

Fig. 10: Recalculated model to illustrate the possible signalling cascade for the induction of GS. The model was validated by a 1000fold recalculation. A gene-to-gene interaction was accepted if it occurred in more than 80 % of the calculations (thick lines). Thin lines represent interactions which were not validated. Dashed lines represent pre-set interactions as the result of first step of robust network search. Solid lines represent interactions determined by the reverse engineering algorithm.

4   Discussion

Glutamine synthetase is expressed in several organs and tissues. In the liver it is located only in a small concentric region surrounding the larger pericentral veins. Periportal hepatocytes do not express GS. The factors involved in the induction of GS in the pericentral regions have been investigated since the early nineties. Using co-cultivation techniques Gebhardt and co-workers [4] demonstrated that a soluble factor is involved. Since the latter is heat and acid labile the authors concluded that it might be a polypeptide. In fact, the factors of the Wnt/β-catenin pathway are soluble and secreted and there is experimental evidence that the Wnt/β-catenin pathway is involved in the regulation of GS expression [13]. It has been shown that mutations in β-catenin can result in GS positive hepatocellular carcinomas [3]. Therefore, one might conclude that the soluble factors described by Gebhardt and co-workers [4] are factors of the Wnt/β-catenin pathway.
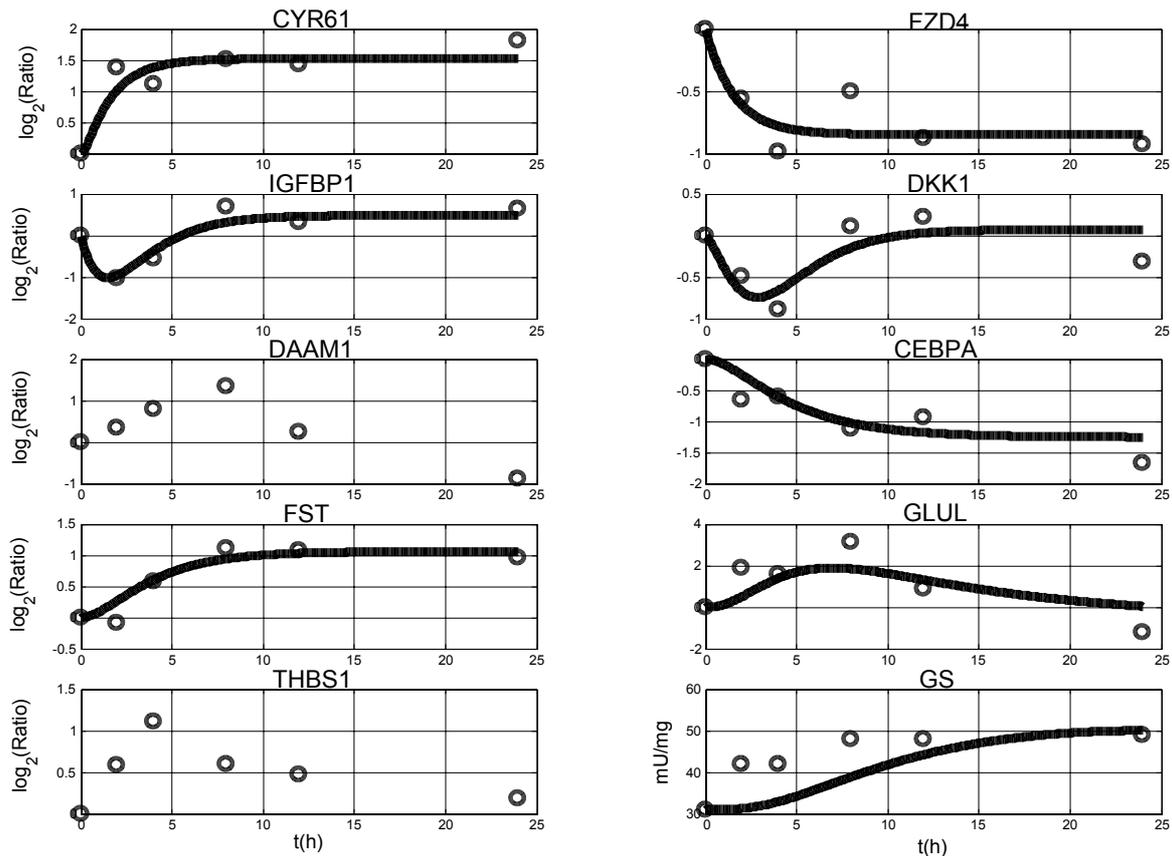
Figure 11: Measured (dots) and simulated expression kinetics (lines; simulation result of the reduced model shown in Fig. 10 considering only the stable interactions validated by recalculations) for the selected genes as well as the specific GS activity.

In the present study the Wnt/β-catenin pathway was activated by inhibition of GSK3β using LiCl and the effect on the specific GS activity was investigated. Using gene chip analysis the change in significantly expressed genes was studied. Incubation of HepG2 cells with 50 mM LiCl for 24 h was not toxic (Fig. 1). However, at 100 mM changes in the morphology occurred. The toxic effects detectable at concentrations above 125 mM are most likely due to osmotic stress.

Incubation of the cells with LiCl resulted in an increase of the specific GS activity, which was also detectable on the mRNA level, using gene chip analysis (Fig. 4). This increase was confirmed by Northern Blot analysis (to be published in an up-coming paper). Since the maximum of the expression is reached after 8-12 h a signalling cascade involving several factors seems likely.

In order to elucidate factors involved in the signalling cascade and their interaction a network was constructed (Fig. 8), based on the data of the gene chip analysis. The corresponding mathematical formulas are shown in Box 1. Known factors of the Wnt/β-catenin pathway and known regulators of GS expression were used as representative genes.

The generated network showed that Dickkopf-1 (DKK-1) has an inhibitory effect on GS expression. Application of the reverse engineering algorithm proved that this interaction is stable and therefore very likely (Fig. 10).

This result is supported by data from literature. It is well known that DKK-1 is a secreted antagonist of the Wnt signalling pathway [14]. Consequently, a decrease in DKK-1 allows for an activation of the canonical Wnt/β-catenin pathway. Results from our laboratory on hepatocytes support these findings. We could demonstrate that secreted DKK-1 inhibits the

expression of GS (to be published in an upcoming paper). Therefore, the model presented in this work predicted a yet unknown interaction between GS and a factor of the Wnt/β-catenin pathway. It also shows that secreted factors, postulated by Gebhardt and co-workers [4] can modulate the expression of GS.

In order to test the stability of the generated network (Fig. 8 and Box 1) the reverse engineering algorithm was applied 1000 times. Fig. 10 shows that 6 gene-to-gene interactions are stable and are thus very likely involved in the signalling cascade that regulates the expression of GS. Besides DKK-1 the model shows that another soluble and secreted factor, IGFBP1, is most likely involved in the regulation of GS. This is supported by data of Finlay and co-workers [15] who demonstrated that LiCl inhibited the GSK3β, which resulted in a decrease of IGFBP1. The model in Fig. 10 indicates that this inhibitory function is also present in HepG2 cells.

Another factor in the model is Cyr61, which is involved in the activation of the Wnt/β-catenin pathway [16]. The experimental data and the model (Fig. 10) show that Cyr61 is up-regulated immediately after the addition LiCl. However, Cyr61 has no stable connection to other factors of the network, indicating that it is most likely not involved in the regulation of GS. This is supported by the data of Latinkic et al. [16], who showed that Cyr61 has a modulating function on the Wnt/β-catenin pathway.

Similar conclusions can be drawn for the genes represented by C/EBPα, which are significantly down-regulated between 8 and 24 h after the addition of LiCl (Fig. 9). Hadden and co-workers [17] reported that C/EBPα has the capacity to activate GS gene transcription. However, the authors concluded from their data that C/EBPα is not sufficient to activate GS and proposed that a second factor is necessary. This might be reflected by the position of CEBPα within the network (Fig. 10).

Finally, one has to keep in mind that other signalling pathways could be involved in the regulation of GS expression. In this work changes on the mRNA level were investigated. Phosphorylation and dephosphorylation of proteins, important components in signalling pathways are not detected. Therefore the network may represent only a fraction of the naturally occurring induction of the GS induction.

Analysis of the presented data using the Kegg pathway showed that several genes of the MAPK pathway are up- or down regulated within the first hours. These are jun D (jun D proto-oncogene), EGFR (epidermal growth factor receptor), DUSP6 (dual specificity phosphatase 6), PRKCBP1 (protein kinase C binding protein 1) and caspase 8. In addition factors of the cell cycle are differentially expressed, including the CDKN1B (cyclin-dependent kinase inhibitor) and genes of the phosphatidylinositol pathway including INPP1 (inositol polyphosphate-1-phosphatase).

Further experimental studies are necessary to prove, which of the above mentioned factors are involved in the regulation of the expression of GS and which are differentially expressed due to effects of LiCl on other regulatory pathways.

5   Acknowledgements:

6   References

[1]   R. Gebhardt. Metabolic zonation of the liver: regulation and implications for liver function. Pharmac. Ther., 53:275–354, 1992.

[2]   S. Colnot, T. Decaens, M. Niwa-Kawakita, C. Godard, G. Hamard, A. Kahn, M. Giovannini, C. Perret. Liver-targeted disruption of Apc in mice activates beta-catenin signaling and leads to hepatocellular carcinomas. Proc. Natl. Acad. Sci. U S A., 101:17216-17221, 2004.

[3]   S. Loeppen, D. Schneider, F. Gaunitz, R. Gebhardt, R. Kurek, A. Buchmann, M. Schwarz. Overexpression of glutamine synthetase is associated with β-catenin-mutations in mouse liver tumors during promotion of hepatocarcinogenesis by phenobarbital. Cancer Research, 62:5685–5688, 2002.

[4]   R. Gebhardt, F. Gaunitz, D. Mecke. Heterogeneous (positional) expression of hepatic glutamine synthetase: features, regulation and implications for hepatocarcinogenesis. Advan. Enzyme Regul., 34:27-56, 1994.

[5]   M. Kruithof-de Julio, W. T. Labruyere, J. M. Ruijter, J. L. M. Vermeulen, V. Stanulovic, J. M. P. Stallen, A. Baldysiak-Figiel, R. Gebhardt, W. H. Lamers, T. B. M. Hakvoort. The RL-ET-14 cell line mediates expression of glutamine synthetase through the upstream enhancer/promoter region. Journal of Hepatology, 43:126–131, 2005.

[6]   F. M. Ausubel, R. Brent, R. E. Kingston, D. D. Moore, J. G. Seidman, J. A. Smith et al.. Current protocols in molecular biology. John Wiley & Sons, Inc., 2004.

[7]   L. Levintow. The glutamyltransferase activity of normal and neoplastic tissues. J. Natl. Cancer, 15:347-352, 1954.

[8]   R. Gebhardt, G. M. Williams. Amino acid transport in established adult rat liver epithelial cell lines. Cell Biol. Toxicol., 2:9-20, 1986.

[9]   M. M. Bradford. A rapid and sensitive method for the quantification of microgram quantities of protein utilizing the principle of protein-dye binding. Anal. Biochem., 72:248-253, 1976.

[10]   R. C. Gentleman, V. J. Carey, D. M. Bates, B. Bolstad, M. Dettling, S. Dudoit, B. Ellis, L. Gautier, Y. Ge, J. Gentry, K. Hornik, T. Hothorn, W. Huber, S. Iacus, R. Irizarry, F. Leisch, C. Li, M. Maechler, A. J. Rossini, G. Sawitzki, C. Smith, G. Smyth, L. Tierney, J. Y. Yang, J. Zhang. Bioconductor: open software development for computational biology and bioinformatics. Genome Biology, 5:R80, 2004.

[11]   B. Bolstad. affyPLM: Methods for fitting probe level models to Affy data. http://www.bioconductor.org/repository/devel/vignette/affyPLM.pdf.

[12]   R. Guthke, U. Möller, M. Hoffmann, F. Thies, S. Töpfer. Dynamic network reconstruction from gene expression data applied to immune response during bacterial infection. Bioinformatics, 21:1626–1634, 2005.

[13]   A. Cadoret, C. Ovejero, B. Terris, E. Souil, L. Levy, W. H. Lamers, J. Kitajewski, A. Kahn, C. Perret. New targets of β-catenin signaling in the liver are involved in the glutamine metabolism. Oncogene, 21:8293–8301, 2002.

[14]   Y. Kawano, R. Kypta. Secreted antagonists of the Wnt signalling pathway. Journal of Cell Science, 116:2627-2634, 2003.

[15]   D. Finlay, S. Patel, L. M. Dickson, N. Shpiro, R. Marquez, C. J. Rhodes, C. Sutherland. Glycogen synthase kinase-3 regulates IGFBP-1 gene transcription through the thymine-rich insulin response element. BMC Mol. Biol., 5:15, 2004.

[16]   B. V. Latinkic, S. Mercurio, B. Bennett, E. M. Hirst, Q. Xu, L. F. Lau, T. J. Mohun, J. C. Smith. Xenopus Cyr61 regulates gastrulation movements and modulates Wnt signalling. Development, 130:2429-2441, 2003.

[17]   T. J. Hadden, C. Ryou, L. Zhu, R. E. Miller. CAAT/enhancer binding protein activates an enhancer in the glutamine synthetase distal 5'-flanking sequence. Arch. Biochem. Biophys., 397:258-61, 2002.